Title
DYNAMICS AND CLUSTERIZATIONIN NUCLEAR COLLISIONS

Authors
Sneppen, K.
Vinet, L.

Publication Date
1987-08-01

LBL-23871 c.2
Preprint

Lawrence Berkeley Laboratory
UNIVERSITY OF CALIFORNIA

Submitted to Nuclear Physics A

Dynamics and Clusterization in Nuclear Collisions

K. Sneppen and L. Vinet

August 1987

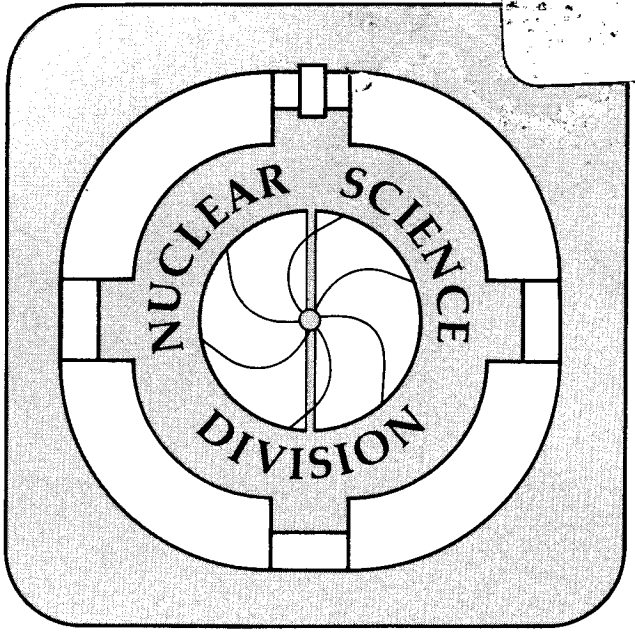

Prepared for the U.S. Department of Energy under Contract DE-AC03-76SF00098

DISCLAIMER

LBL-23871

DYNAMICS AND CLUSTERIZATION IN NUCLEAR COLLISIONS

K. Sneppen [1] and L. Vinet [2]

Nuclear Science Division, Lawrence Berkeley Laboratory,

University of California, Berkeley, CA 94720

August 26, 1987

Abstract

Collisions of two nuclei for bombarding energies between 20 and 100 MeV/A are investigated by combining the Landau-Vlasov equation with a statistical fragmentation approach. The stage of a possible clusterization appears to be strongly dependent on the energy, such that the fragmentation occurs at a nearly invariant temperature (T$\approx$ 6–7 MeV). Including conservation of total angular momentum we examine the competition between evaporation, fission and multifragmentation as a function of bombarding energies and impact parameters.

1 Introduction

Various theoretical approaches have recently been developed to predict the outcome of nuclear collisions at intermediate energies (20–100 MeV/A). Until now, most of the models only consider a given excited nucleus, ignoring the effects of the entrance channel. For instance, an equilibrium assumed by statistical models [1–11] will depend on the system involved, the beam energy and the impact parameter [12]. On one hand, such effects are clearly seen by the one-body Landau-Vlasov (LV) description [13–16] . However, this LV equation cannot correctly represent the decay

[1]Permanent address: Niels Bohr institute, Blegdamsvej 17, DK-2100, Copenhagen, Denmark

[2]Present address: CERN European Organization For Nuclear Research, CH-1211 Geneva 23, Switzerland

of nuclei, because of the lack of many-body correlations. On the other hand, the statistical approaches take into account, in principle, all the possible fluctuations within the available phase space. These last models form two classes differentiated by the way of decay. The ones from the first class [1–3] only allow sequential emission of fragments, but treat the saddle point carefully, whereas the others [4–11] consider also a simultaneous break up of the system (multifragmentation).

The sequential emission models are in good agreement with experimental data at low energies, but, at high energies, they might fail due to the competition with complex decay channels. The multifragmentation models suffer from the unknown "multidimensional saddle point" or freeze-out criteria. The LV calculation will show later that the dynamical evolution of a nuclear collision at high energies leads to densities and temperatures where the liquid-gas phase transition becomes important. Thus the final clusterization pattern must be appropriately described by a multifragmentation model which takes into account the proper degrees of freedom for the inhomogeneous liquid-gas mixture.

In the present paper, the LV equation solved with a coherent state basis [13] will provide us with a well defined freeze-out volume. Then using the liquid-drop parametrization of the phase space given by [5], we show how a general rotation of the system can be included. Thus, we will be able to take account of non-central collisions where a single equilibrated source prevails. This will allow us to compare with experiments down to relatively low energies.

2 The Landau-Vlasov approach to the freeze-out density

The early stages of an intermediate energy nuclear collision can be reasonably well described by the LV equation [13,16]

$$\frac{\partial f}{\partial t} + \frac{\mathbf{p}}{m}\frac{\partial f}{\partial \mathbf{r}} - \frac{dV}{d\mathbf{r}}\frac{\partial f}{\partial \mathbf{p}} = I_{coll}. \tag{1}$$

This equation governs the evolution of the one-body phase space density $f = f(\mathbf{r}, \mathbf{p}, t)$ self-consistently in its own mean field potential

$$V(\mathbf{r}) = -d_1 \frac{\rho(\mathbf{r})}{\rho_0} + d_2 \left(\frac{\rho(\mathbf{r})}{\rho_0} \right)^{\frac{7}{6}} + V_{coul}(\{\rho(\mathbf{r})\}) \tag{2}$$

where $\rho(\mathbf{r}, t) = \int f(\mathbf{r}, \mathbf{p}, t)\, d\mathbf{p}$ is the spatial density and $d_1 = 368.3$ MeV, $d_2 = 315.2$ MeV. Thus V is determined as a sum of a Skyrme-type interaction (with saturation density $\rho_0 = 0.15$ fm^{-3}, compressibility $K = 200$ MeV and critical temperature $T_c = 16$ MeV) and the Coulomb interaction. Equation (1) furthermore includes the Uehling-Uehlenbeck collision integral I_{coll} which takes into account two body correlations. The equation is solved by decomposing the density f onto a finite basis of gaussians which initially is randomly distributed in the phase space determined by the Thomas-Fermi approximation [13]. The width of these gaussians are defined such that the surface diffuseness and binding energy of the nuclei fit the experimental ones.

At these intermediate energies, central collisions lead to a highly excited compound system. The evolution of such a system has been intensively studied [17–20]. It turns out that the limit of stability depends on the mode of excitation. Thus a ^{40}Ca nucleus needs 15 MeV/A of thermal energy to disintegrate whereas it only needs 8 MeV/A of compressional energy [18]. The conclusion of this LV study has shown that the limit of stability of nuclear matter is rather high. To understand the reason for this stability we have to emphasize two points. First the evaporation of particles, which is favored by the collision term, removes energy from the remaining system. This slows down the collective expansion of the system. For an equilibrated nucleus this evaporation turns out to be bigger than predicted by statistical models which assume evaporation rates proportional to an inverse cross section. Secondly, by construction the LV equation only considers the average evolution of the system. Therefore it does not, in principle, initiate any fluctuations during the evolution of the system. Nevertheless, due to the finite number of gaussians and to the numerical

resolution of the LV equation, fluctuations are present. Those should be minimized, so that the main pattern of the evolution of a system remains independent of further increase in the accuracy of the calculation [18].

In this paper, instead of considering an excited compound system, where the form of excitation is arbitrary, we prefer to follow a system from the beginning of the collision. Figure 1 shows such a collision between two ^{40}Ca nuclei at 60 MeV/A. The collision initiates a compression to a density $\rho \approx 1.4\rho_0$, as shown in figure 2b, followed by a general expansion phase. During the expansion particles are continuously emitted into the continuum as shown in figure 2c where the size of the remaining system is displayed. From 80 fm/c some fluctuations start to grow on a macroscopic scale and the system finally clusterizes. At lower laboratory energies ($E_{lab} < 50$ MeV/A) the pattern of evolution is different. The numerical fluctuations never grow on a macroscopic scale, and therefore do not play any role, so the system finally recompresses to a compound system as shown in figure 2b for $E_{lab} = 40$ MeV/A. However, the fluctuations present in the LV study do not fully represent reality.

If the system ever gets to an equilibrium the fluctuations would be such that the system maximizes its entropy. During the expansion phase it is not in equilibrium. Energy is continuously transferred from translational to potential energy. As shown by figure 2a, the potential energy per nucleon evolves through a maximum. This characterizes either the end of an expansion or the beginning of a clusterization. In the first case, the system should have sufficient time to explore the available phase space, but here the LV equation is unable to provide the necessary fluctuations to do that. In the second case the situation is opposite. The fluctuations are amplified by the dynamical instability of the matter. This does not mean that the phase space is isotropically explored. The solution in such a case could be an average of a sequence of calculations with different initial fluctuations [21,22]. But it turns out that the final clusterization pattern is very dependent of the initial fluctuations [18] which are not presently clearly defined. In both cases we therefore treat the final evolution of the system statistically at the stage of maximum potential energy per nucleon. Figure 3 displays the nuclear profile for different energies at this stage and table 1

gives the corresponding central density, mass number and excitation energy of the remaining system. We thereby define the freeze-out conditions that statistical models need as input [7,9,11].

We would like to emphasize that the freeze-out density found by the LV approach depends very much on the bombarding energy per nucleon and the relative sizes of the two colliding nuclei. At freeze-out the homogeneous matter typically has a thermal energy corresponding to a temperature $T \approx 3 - 5$ MeV. For higher temperatures, possible disruptions of the matter are suppressed by the thermal motion of its constituents. With the freeze-out densities of table 1, a temperature $T \approx 3 - 5$ MeV defines the matter to be within the spinodal region of the phase diagram when E_{lab} is above 20 MeV/A (for the potential given by eq.(2) $\frac{dP}{d\rho}|_{S=0} = \frac{dP}{d\rho}|_{T=0}$ is negative for $0.001 < \rho/\rho_0 < 0.626$). Thus the freeze-out conditions can be understood from a long-wavelength decomposition of the matter, taking into account that clusterization occurs at constant energy (where density fluctuations can only develop at temperatures $T \lesssim 9$ MeV [23,24]), and that fluctuations need to be of a finite size $\lambda \gtrsim 5$ fm in order to grow [25,26]. This last condition also implies that a fluctuation needs a finite time $\tau \approx \lambda/v_{fermi} \approx 20$ fm/c in order to manifest itself on a macroscopic scale, thereby initiating the clusterization process.

Investigating the amount of energy which is fully thermalized we also show, in table 1, the size of the average radial motion at freeze-out. The size of the radial kinetic energy makes it reasonable to assume equipartition of all available energy when the bombarding energy is below 70 – 80 MeV/A. It also indicates the transition between recompression and continuous expansion, of the system described by the LV equation, located around 50 MeV/A. The following chapter will describe the statistical weight of various final fluctuation patterns of the system, taking into account that the total energy, momentum and angular momentum have to be conserved.

3 Phase space description of a rotating liquid-gas mixture

In the first part the LV approach has provided us with a freeze-out stage at which we, now, assume thermodynamic equilibrium. We can then use the statistical multifragmentation model of Bondorf et al. [5,7]. Here we improve the model so that the Coulomb repulsion and the hard-sphere blocking are calculated explicitly by placing the fragments randomly within the freeze-out volume. This also allows this volume to be non-spherical. Furthermore, and most important, we take into account a possible rotation of the system.

A specific fragmentation mode of the system is defined by a partition vector $\{N_{A,Z}\} = \{N_{1,0},\ N_{1,1},\ N_{2,0},...\}$ where $N_{n,l}$ denotes the number of fragments with mass n and charge l. Given a total angular momentum $\mathbf{L}\hbar$ and a total energy E, the statistical weight of a partition is defined as

$$\begin{aligned} W\left(\{N_{A,Z}\},E,\mathbf{L}\right) = \ & \frac{1}{\Pi N_{A,Z}!}\int_{\Omega} h^3 \prod_{i=1}^{M} \frac{d^3\mathbf{r}_i d^3\mathbf{p}_i}{h^3} d\epsilon_i \rho\left(\epsilon_i\right) \delta^3\left(\textstyle\sum_i \mathbf{p}_i\right) \delta^3\left(\textstyle\sum_i m_i \mathbf{r}_i\right) \\ & \textstyle\sum_{\mathbf{s}_1,\mathbf{s}_2...\mathbf{s}_M} \delta^3\left(\mathbf{L}\hbar - \sum_i \left(\mathbf{r}_i \times \mathbf{p}_i + \mathbf{s}_i\hbar\right)\right) \\ & \delta\left(E - V - \textstyle\sum_i \left(\frac{\mathbf{p}_i^2}{2m_i} + \frac{\mathbf{s}_i^2\hbar^2}{2j_i} + \epsilon_i\right)\right) \end{aligned} \tag{3}$$

where $V = V\left(\{N_{A,Z}^i, \mathbf{r}_i\}\right)$ is the total potential energy of the partition and Ω denotes the volume available for the fragments (the volume at which the center-of-mass of each fragment could be positioned). The index i runs over all the fragments, $\rho\left(\epsilon_i\right)$ is the energy level density of the fragment i having an internal energy ϵ_i. The variables $\mathbf{s}_i$ and j_i are respectively the angular momentum and the moment of inertia of the fragment i that we treat as a classical sphere. $\frac{1}{\Pi N_{A,Z}!}$ takes into account the double counting of the phase space in case of identical fragments.

Using the transformation $\mathbf{p}_i \rightarrow \mathbf{p}_i - m_i\omega \times \mathbf{r}_i$; $\mathbf{s}_i \rightarrow \mathbf{s}_i - m_i\omega j_i$, with $\omega = \mathbf{L}/J$, $J = \sum_i (j_i + m_i\mathbf{r}_{i\perp}^2)$, the integral will be expressed in a convenient rotating frame. With a canonical limit corresponding to the one used in reference [7], the integral then reads

$$W\left(\{N_{A,Z}\},E,\mathbf{L}\right) = \frac{h^3}{\Pi N_{A,Z}!}\int_\Omega \left(\prod_i d^3\mathbf{r}_i\right)\delta^3\left(\sum_i m_i\mathbf{r}_i\right)\int\prod_i \frac{d^3\mathbf{p}_i}{h^3}e^{-\frac{\mathbf{p}_i^2}{2m_iT}-\frac{F_i(T)}{T}}\delta^3\left(\sum_i \mathbf{p}_i\right)$$

$$\sum_{\mathbf{s}_1,\mathbf{s}_2\ldots\mathbf{s}_M}\delta^3\left(\sum\left(\mathbf{r}_i\times\mathbf{p}_i+\mathbf{s}_i\hbar\right)\right)e^{-\sum_i\frac{\mathbf{s}_i^2\hbar^2}{2j_iT}}e^{\left(E-V-\frac{L^2\hbar^2}{2J}\right)/T} \quad (4)$$

where $T=T\left(\{N^i_{A,Z},\mathbf{r}_i\}\right)$ is the temperature determined such that the total energy in the rotating frame is conserved and $F_i=-T\ln\left[\int d\epsilon_i\rho\left(\epsilon_i\right)e^{-\epsilon_i/T}\right]$ the internal free energy of fragment i. For simplification, the rotation of the fragments will only be considered in the reaction plane. Thus in the following, we only consider conservation of angular momentum along the z axis. With the saddle point approximation

$$\sum_{s_1,\ldots s_M}\delta\left(\sum_i\left(\left(\mathbf{r}_i\times\mathbf{p}_i\right)_z+s_i\hbar\right)\right)e^{-\sum\frac{s_i^2\hbar^2}{2j_iT}}\approx\sum_{s_1,\ldots s_M}\delta\left(\sum_i s_i\right)e^{-\sum\frac{s_i^2\hbar^2}{2j_iT}}e^{-\frac{\left(\sum\mathbf{r}_i\times\mathbf{p}_i\right)_z^2}{2\sum j_iT}} \quad (5)$$

the statistical weight can be evaluated

$$W\left(\{N_{A,Z}\},E,\mathbf{L}\right)\approx\int_\Omega\frac{\left(\prod_i\frac{d^3\mathbf{r}_i}{\Omega}\right)\delta^3\left(\sum_i m_i\mathbf{r}_i\right)}{\Pi N_{A,Z}!}e^{\left(E-V-\frac{L^2\hbar^2}{2J}\right)/T}$$

$$\frac{\prod_i\left[\Omega\left(\frac{2\pi m_iT}{h^2}\right)^{3/2}\left(\frac{2\pi j_iT}{\hbar^2}\right)^{1/2}e^{-F_i(T)/T}\right]}{\left(\frac{2\pi\sum_i m_iT}{h^2}\right)^{3/2}\left(\frac{2\pi\sum_i\left(m_i\mathbf{r}_{i\perp}^2+j_i\right)T}{\hbar^2}\right)^{1/2}}. \quad (6)$$

In this equation the free energy of the fragment (A,Z) is

$$F_{A,Z}\left(T\right)=f_{bulk}\left(T\right)A+f_{surf}\left(T,T_c\right)A^{2/3}+f_{asym}\left(A,Z\right)+\frac{3}{5}\frac{Z^2e^2}{r_0A^{1/3}} \quad (7)$$

where $f_{bulk}\left(T\right)$, $f_{surf}\left(T,T_c\right)$ and $f_{asym}\left(A,Z\right)$ are determined by the parameters of the liquid-drop model used in ref [5,27] (with $T_c=16$ MeV). For fragments with mass number $A\leq 4$ we set $F_{A,Z}$ equal to the ground state energy. Given the free energy $F_i=F_i(T)$, the average energy of fragment i at temperature T, can be calculated by $E_i(T)=F_i+TS_i$, where $S_i=-\frac{dF_i}{dT}$ is the internal entropy.

The integral (6) is calculated by a Monte-Carlo method. Thus, in order to calculate the average value of a physical observable Q, we generate randomly a sample of partitions as described in reference [27]. For each partition k, the fragments are placed randomly within the freeze-out volume Ω. The hard-sphere repulsion is taken into account by rejecting partitions where some fragments overlap ($V = \infty$). If the partition is accepted, it is assigned the statistical weight

$$W_k = \frac{1}{\Pi N_{A,Z}!} \frac{\Pi_i \left[\Omega \left(\frac{2\pi e m_i T}{h^2} \right)^{3/2} \left(\frac{2\pi e j_i T}{\hbar^2} \right)^{1/2} e^{S_i(T)} \right]}{\left(\sum_i \left(\frac{m_i}{\sum_j m_j} \right)^2 \right)^{3/2} \Omega \left(\frac{2\pi e \sum_i m_i T}{h^2} \right)^{3/2} \left(\frac{2\pi e J T}{\hbar^2} \right)^{1/2}} \tag{8}$$

where $T = T\left(\{N^i_{A,Z}, \mathbf{r}_i\}\right)$ is determined by

$$E = \frac{L^2\hbar^2}{2J} + \sum_{i>j} \frac{e^2 Z_i Z_j}{|\mathbf{r}_i - \mathbf{r}_j|} + \frac{3}{2}(M-1)T + \frac{1}{2}(M-1)T + \sum_i E_i(T). \tag{9}$$

$M = \sum_{A,Z} N_{A,Z}$ is the multiplicity of the partition $\{N_{A,Z}\}$. The δ–function in the coordinate space is approximately taken into account by the division with the second moment of the mass distribution in eq. 8 and by calculating the total moment of inertia $J = J_z = \sum_i \left(m_i \left(\mathbf{r}_{i\perp} - \frac{\sum m_i \mathbf{r}_{i\perp}}{\sum_i m_i} \right)^2 + j_i \right)$ relative to the center-of-mass of the randomly placed fragments.

The average of an observable Q is calculated over all accepted partitions in the sample by

$$\langle Q \rangle = \frac{\sum_k W_k Q_k}{\sum_k W_k}. \tag{10}$$

The size of the sample is chosen such that the average value does not change when increasing the number of partitions by a factor two. This typically requires 10^5 to 10^6 partitions, according to the size of the system and to the physical observables we want to study.

Figures 4a,b show the influence of the new ingredients of the model on the average temperatures and multiplicities at freeze-out. For no angular momentum one observes that the explicit treatment of the hard-sphere blocking causes a slight increase of the temperature. The inclusion of the internal rotational degree of freedom of the fragments only plays a minor role. The introduction of a finite total angular momentum L enhances the average size of the fragments so much that the temperature at freeze-out stays relatively unchanged, except at low energy where a large fraction of the energy is involved in the rotational motion. The inclusion of a finite angular momentum also favors the fission channel as described by Figure 5. The fission probability depends very much on the total excitation energy of the system as well as on the size of the freeze-out volume. Therefore it is very important that these two last quantities are well defined when one wants to compare with experiments.

4 Fragmentation pattern in nuclear collisions

Having the freeze-out density given by the LV approach in chapter 2, we have to define the corresponding freeze-out volume available to the fragments in the statistical model of multifragmentation described in chapter 3. For the volume $V = A/\rho$ where A is the mass of the system at freeze-out, the question remains whether one should place the fragments totally within this volume [11] or one should allow the center-of-mass of the fragments at the periphery of this same volume [9]. This problem is of less importance at high energies (above $\approx$ 50 MeV/A for Ca + Ca), where the fragments are small and the volume big, but at low energies it plays an important role. Thus, for the system ^{40}Ca(30 MeV/A) + ^{40}Ca at freeze-out, the average multiplicity (resp. the probability that the biggest fragment contains more than $\frac{2}{3}$ of the total number of nucleons) is 3.0 (resp. 0.85) for the first choice, and 5.0 (resp. 0.01) for the second case. As we have a rather broad density profile, it does not seem reasonable to choose the fragments totally inside the volume V. Moreover, at low energies the center of big fragments should not be at the periphery of V. In the following, we choose the intermediate solution, where each fragment center is allowed to be placed till half

its radius from the border of the previous volume V. We will see later that this alternative gives results in agreement with experimental data.

In order to understand the influence of the incident energy on the fragmentation process, we are first going to study the central collisions ($b = 0$ fm). Figures 6a,b display the multiplicity and the temperature versus the beam energy for the system Ca + Ca. The temperature stays fairly constant with the involved energy, which is not the case of the figure 4 where the freeze-out volume is kept constant. As shown previously in table 1, the freeze-out volume increases dramatically with the beam energy. This enhances the multiplicity, but with more fragments, less thermal energy is available per degree of freedom. The same behaviour is observed with the freeze-out criteria of Bondorf et al. [6] which assumes an explicit dependence of the freeze-out volume on the multiplicity.

For non-central collisions, LV gives a spheroidal freeze-out volume and a higher total excitation energy because of a lower pre-equilibrium emission. Figure 7 shows two different and typical behaviours according to the impact parameter. For $b = 1$ fm the system ^{40}Ca(40 MeV/A) + ^{40}Ca behaves as a thermal equilibrated source at the freeze-out stage, whereas for $b = 3$ fm the distribution of the velocities can only be explained by the presence of two sources. The energies and impact parameters where we have one or several equilibrated sources are summarized in figure 8. The energy region below 15 MeV/A limits the validity of our approach. The intermediate area states the uncertainty between the two phenomena.

The one-source case forms a highly excited compound system, with more or less angular momentum, whose decay can be investigated by the presently described multifragmentation model. For ^{40}Ca + ^{40}Ca, table 2a and 2b present the explicit dependence of the excited source on the impact parameter for two laboratory energies E_{lab} = 20 MeV/A and 30 MeV/A. The freeze-out density remains more or less constant whereas the excitation energy increases significantly for the highest impact parameter, indicating a transition towards a deep inelastic reaction. Due to these freeze-out conditions the multiplicity (Fig. 9a) and the temperature (Fig. 9b) are not much influenced by the impact parameter while the decay mode (Fig. 9c, 9d)

manifests a very sensitive behaviour. These two last figures also reveal an onset of multifragmentation located around 25 MeV/A of bombarding energy for the system ^{40}Ca + ^{40}Ca.

In absence of relevant experimental data at high energies, we have compared the outcome of our approach with some experiments at lower energies. The experimental data are provided by [28] where charge yield distributions resulting from the decay of one excited source are extracted. The comparison of these distributions with our approach in Figures 10a,b shows a reasonable agreement for ^{40}Ar(20 MeV/A) + ^{27}Al, where the excitation energy of the excited source is approximately 4 MeV/A. The comparison for the system ^{40}Ar(20 MeV/A) + ^{12}C demonstrates the limit of our approach at low excitation energies (2.5–3.0 MeV/A), where the detailed structure of the saddle point is deficient.

5 Conclusion

In the present paper, the Landau-Vlasov equation has shown, that near-central nuclear collisions lead to a stage of freeze-out at which clusterization could occur. Since many-body correlations are neglected in this LV formalism, the phase space of the liquid-gas mixture at freeze-out is described statistically by the multifragmentation model of [5,7] improved in order to take into account a possible rotation of the system. The freeze-out volume appears to increase strongly with the bombarding energy, entailing the temperature at freeze-out to stay around 6–7 MeV for the system Ca + Ca where 15 MeV/A $< E_{lab} <$ 80 MeV/A.

In general, one observes a gradual change of decay ranging from sequential evaporation at low energies ($E_{lab} <$ 20 MeV/A), through fission at intermediate energies to pure fragmentation at high energies ($E_{lab} >$ 35 MeV/A). The fission-like channel is enhanced by a rotation of the source, and hence becomes important with increased impact parameter of the collision. Averaging over the impact parameters at which one can expect one source, we finally have compared our calculations with experimental data at energies where evaporation and fission take place.

Acknowledgement

The authors would like to thank G. Fai, A. Moroni, J. Randrup and G. Wozniak for a careful reading of the manuscript, and the Nuclear Science Division at the Lawrence Berkeley Laboratory for its hospitality.

This work was supported by the director, Office of Energy Research, Division of Nuclear Physics of the Office of High Energy and Nuclear Physics of the U.S. Department of Energy under Contract DE-AC03-76SF00098.

References

[1] V. Weisskopf, Phys. Review. **52** (1937) 295.

[2] L.G. Moretto, Nucl. Phys. **A247** (1975) 211.

[3] W.A. Friedman and W.G. Lynch, Nucl. Phys. **A247** (1975) 211.

[4] J.P. Bondorf, Nucl. Phys. **A430** (1984) 445.

[5] J.P. Bondorf, R. Donangelo, I.N. Mishustin, C.J. Pethick, H. Schulz and K. Sneppen, Nucl. Phys. **A443** (1985) 321.

[6] J.P. Bondorf, R. Donangelo, I.N. Mishustin, C.J. Pethick and K. Sneppen, Phys. Lett. **150B** (1985) 57.

[7] J.P. Bondorf, R. Donangelo, I.N. Mishustin and H. Schulz, Nucl. Phys. **A444** (1985) 460.

[8] J. Randrup and S.E. Koonin, Nucl. Phys. **A356** (1981) 223.

[9] J. Randrup and S.E. Koonin, Preprint Map–87, Nucl. Phys. **A** (1987) in press.

[10] D.H.E. Gross, Phys. Lett. **161B** (1985) 47.

[11] Zhang Xiao-Ze, D.H.E. Gross, Xu Shu-yan and Zheng Yu-Ming, Nucl. Phys. **A461** (1987) 641, and Nucl. Phys. **A461** (1987) 668.

[12] G. Fai and J. Randrup, Nucl. Phys. **A404** (1983) 551, Comp. Phys. Comm. **42** (1986) 385.

[13] C. Gregoire, B. Remaud, F. Sebille, L. Vinet and Y. Raffray, Nucl. Phys. **A465** (1987) 317.

[14] B. Remaud, C. Gregoire, F. Sebille and L. Vinet, Phys. Lett. **180B** (1986) 198.

[15] C. Gregoire, B. Remaud, F. Sebille and L. Vinet, Phys. lett. **186B** (1987) 14.

[16] J. Aichelin and G.F. Bertsch, Phys. Rev. **C31** (1985) 1730.

[17] L. Vinet, F. Sebille, C. Gregoire, B. Remaud and P. Schuck, Phys. Lett. **172B** (1986) 17.

[18] L. Vinet, C. Gregoire, B. Remaud, F. Sebille and P. Schuck, Nucl. Phys. **A468** (1987) 321.

[19] L. Vinet, These d'Universite, Orsay **160** (1986).

[20] P. Bonche, D. Vautherin and M. Veneroni, J. Phys. (Paris) **C4** (1986) 339.

[21] J. Knoll and B. Strack, Phys. Lett. **149B** (1984) 45.

[22] E. Beauvais, D.H. Boal and J.C.K. Wong, Phys. Rev. **C35** (1987) 545.

[23] A. Vicentini et al. Phys. Rev. **C31** (1985) 1783.

[24] L.P. Csernai and J. Kapusta, Phys. Rep. **131** (1986) 223.

[25] F.F. Abraham, Phys. Reports **53** (1979) 93.

[26] C.J. Pethick and D.G. Ravenhall, Proceedings of the ACS Symposium on central Collisions and Fragmentation Processes, Denver, Colorado, April 5-10, 1987, North Holland, C.K. Gelbke, ed., (in press).

[27] K. Sneppen, Nucl. Phys. **A470** (1987) 213.

[28] E. Plagnol et al., to be published.

Table captions

Table 1 Freeze-out conditions for a range of bombarding energies for central collisions of two ^{40}Ca nuclei.

Table 2a Freeze-out conditions for a range of impact parameters of ^{40}Ca(20 MeV/A) + ^{40}Ca. c/a is a spheroidal parameter which gives the deformation of the homogeneous source whose approximated form is $\left(\frac{x}{a}\right)^2 + \left(\frac{y}{a}\right)^2 + \left(\frac{z}{c}\right)^2 = 1$.

Table 2b Same as Table 2a for ^{40}Ca(30 MeV/A) + ^{40}Ca.

Figure captions

Fig. 1 Time evolution of the central collision ^{40}Ca(60 MeV/A) + ^{40}Ca, calculated with the LV equation. The plots show the integrated density $\rho(x,z) = \int \rho\,(x,y,z)\,dy$.

Fig. 2a Time evolution of the potential energy per nucleon for two central collisions of two Ca nuclei. Note the maximum point indicating the state of maximum homogeneous expansion.

Fig. 2b Same as figure 2a for the central density.

Fig. 2c Same as figure 2a for the size of the remaining system, where the density $\rho(x,z)$ is above $\frac{1}{10}$ of the central ones.

Fig. 3 Stages of maximum homogeneous expansion (or freeze-out) for central collisions of two Ca nuclei at various laboratory energies E_{lab}.

Fig. 4a Average multiplicity as function of the excitation energy for the system (A = 80, Z = 40) at a fixed freeze-out volume $\Omega = 2A_{total}/\rho$ in four cases. The "Old" case refer to the result of the model of Bondorf et al. [5,7] which takes into account the hard-sphere blocking only approximately and neglects any angular momentum effect. The "$L = 0\hbar$","$L = 80\hbar$" and "$L = 120\hbar$" cases correspond to our approach for different values of the total angular momentum L.

Fig. 4b Same as figure 4a for the average temperature at freeze-out.

Fig. 5 Influence of the angular momentum on the fission like decay for different excitation energies ϵ^* and different volumes Ω available for the fragments at freeze-out. The fission probability is, here, defined as the probability that a partition at freeze-out has a second biggest fragment with a mass superior to $\frac{1}{3}$ of the total mass.

Fig. 6a Average multiplicity as function of the laboratory energy E_{lab} for central collisions of two Ca nuclei, before and after a classical secondary

evaporation of light particles (A $\leq$ 4) [1]. Only fragments with masses A > 4 are considered for the case after secondary evaporation. The error bars show the width of the multiplicity distribution.

Fig. 6b Same as figure 6a for the average temperature at freeze-out.

Fig. 7 Same as figure 1, for the system ^{40}Ca(40 MeV/A) + ^{40}Ca at two impact parameters b = 1 fm, 3 fm.

Fig. 8 Impact parameters and laboratory energies where two colliding ^{40}Ca nuclei form one excited source.

Fig. 9a Average multiplicity at freeze-out as function of impact parameter for two different bombarding energies E_{lab} of the colliding ^{40}Ca + ^{40}Ca system.

Fig. 9b Same as figure 9a for the average temperature at freeze-out.

Fig. 9c Influence of the impact parameter on the fission-like, the evaporation-like and the multifragmentation-like decay for two colliding Ca at a laboratory energy E_{lab} = 20 MeV/A. See figure 5 for the definition of the "fission-like", "evaporation-like" means that the biggest fragment at freeze-out has a mass superior to $\frac{2}{3}$ of the total mass and the "multifragmentation" is defined as the residual events. The "multiplicity > 2" case is independently shown to illustrate the importance of simultaneous break up into several fragments.

Fig. 9d Same as figure 9c for a bombarding energy E_{lab} = 30 MeV/A.

Fig. 10a Charge yield comparison between our approach (including a secondary evaporation [1] after the freeze-out) averaged over the impact parameters b = 0, 1,.., 5 fm, and the experiments of the reference [28] for the system ^{40}Ar(20 MeV/A) + ^{12}C.

Fig. 10b Same as figure 10a for the system ^{40}Ar(20 MeV/A) + ^{27}Al where the calculation is averaged over the impact parameters b = 0, 1,.., 4 fm.

$^{40}Ca + {}^{40}Ca$ for b = 0 fm

E_{lab} (MeV/A)	ρ/ρ_o	A	E^* (MeV/A)	E_r (MeV/A)
15	.66 ± .03	73 ± 1	3.2 ± .2	.1
20	.66 ± .03	72 ± 1	4.0 ± .3	.2
30	.49 ± .03	70 ± 2	6.2 ± .4	.3
40	.38 ± .02	69 ± 2	7.7 ± .4	.3
50	.27 ± .02	62 ± 2	8.5 ± .5	1.0
60	.20 ± .02	62 ± 3	10.4 ± .6	1.3
70	.15 ± .02	59 ± 4	11.5 ± .7	2.0
80	.12 ± .01	57 ± 5	12.2 ± 1.0	2.5
100	.07 ± .01	51 ± 5	15.2 ± 1.5	4.4
120	.05 ± .01	48 ± 5	17.1 ± 2.0	6.0

Table 1

$^{40}Ca + {}^{40}Ca$ at 20 MeV/A

b (fm)	ρ/ρ_o	A	E^* (MeV/A)	c / a	L (ħ)
0	.66	72	4.0	0.8	0
1	.66	73	3.9	1.1	18
2	.64	73	3.9	1.3	33
3	.66	73	3.8	1.4	49
4	.66	75	4.2	1.5	67
5	.72	75	4.4	1.7	88

Table 2a

$^{40}Ca + {}^{40}Ca$ at 30 MeV/A

b (fm)	ρ/ρ_o	A	E^* (MeV/A)	c / a	L (ħ)
0	.49	70	6.2	0.8	0
1	.52	71	5.8	1.2	21
2	.50	73	6.0	1.4	43
3	.55	74	6.3	1.6	64
4	.55	75	6.5	1.7	84

Table 2b

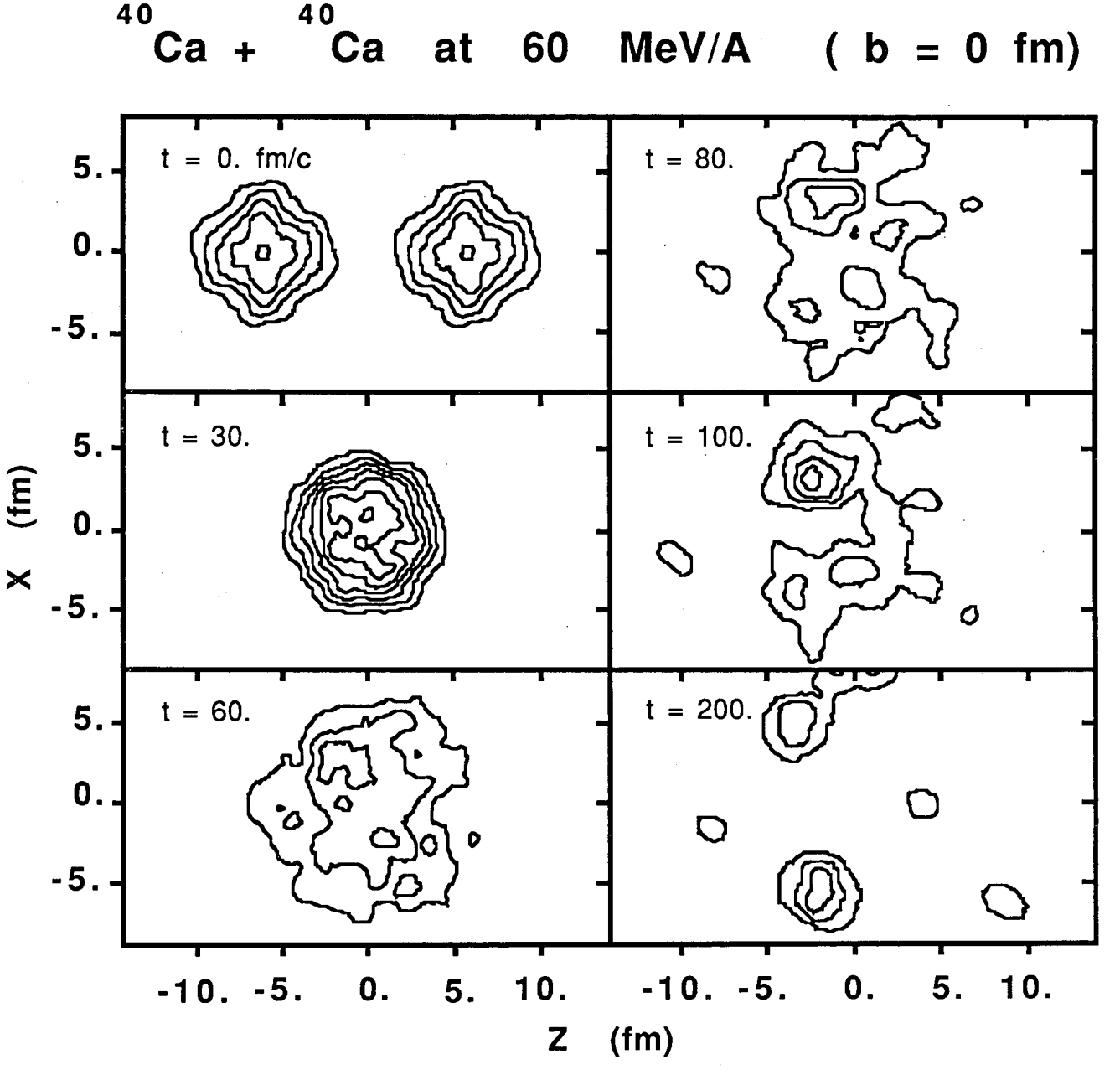
40Ca + 40Ca at 60 MeV/A (b = 0 fm)
t = 0. fm/c
t = 80.
t = 30.
t = 100.
t = 60.
t = 200.
5.
0.
-5.
X (fm)
-10. -5. 0. 5. 10.
Z (fm)

Figure 1

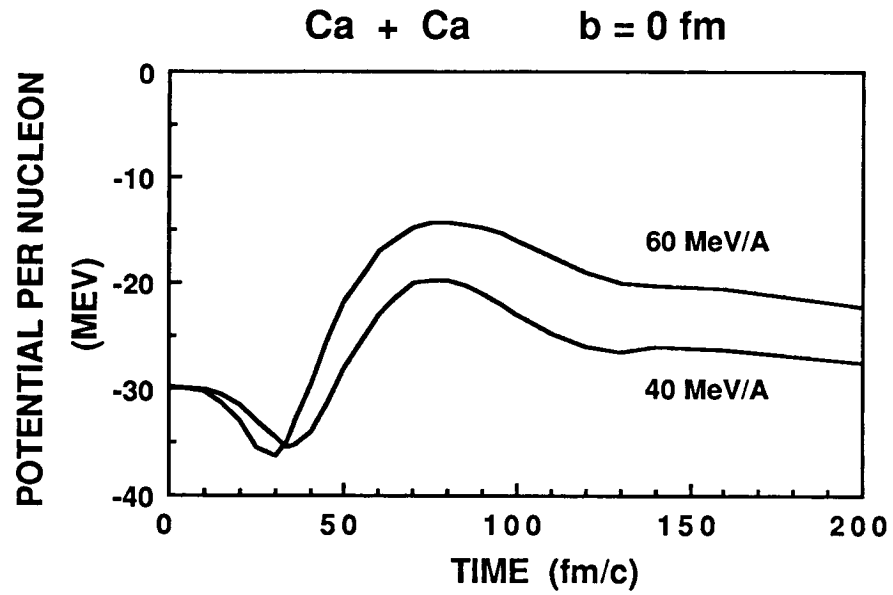

Figure 2a

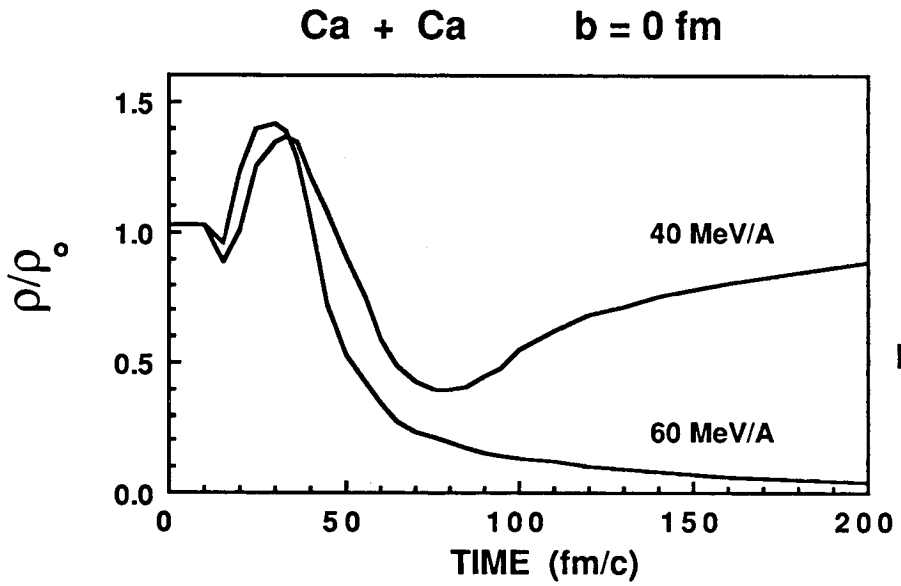

Figure 2b

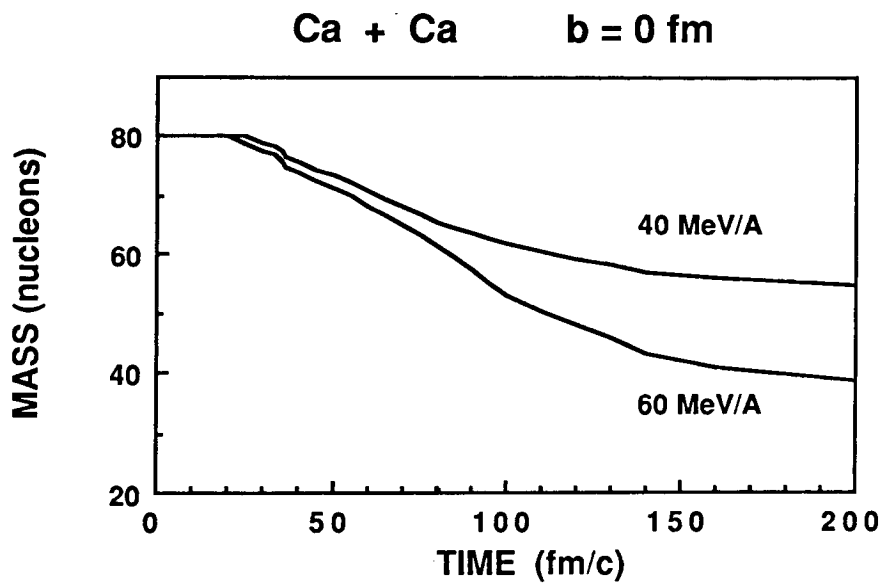

Figure 2c

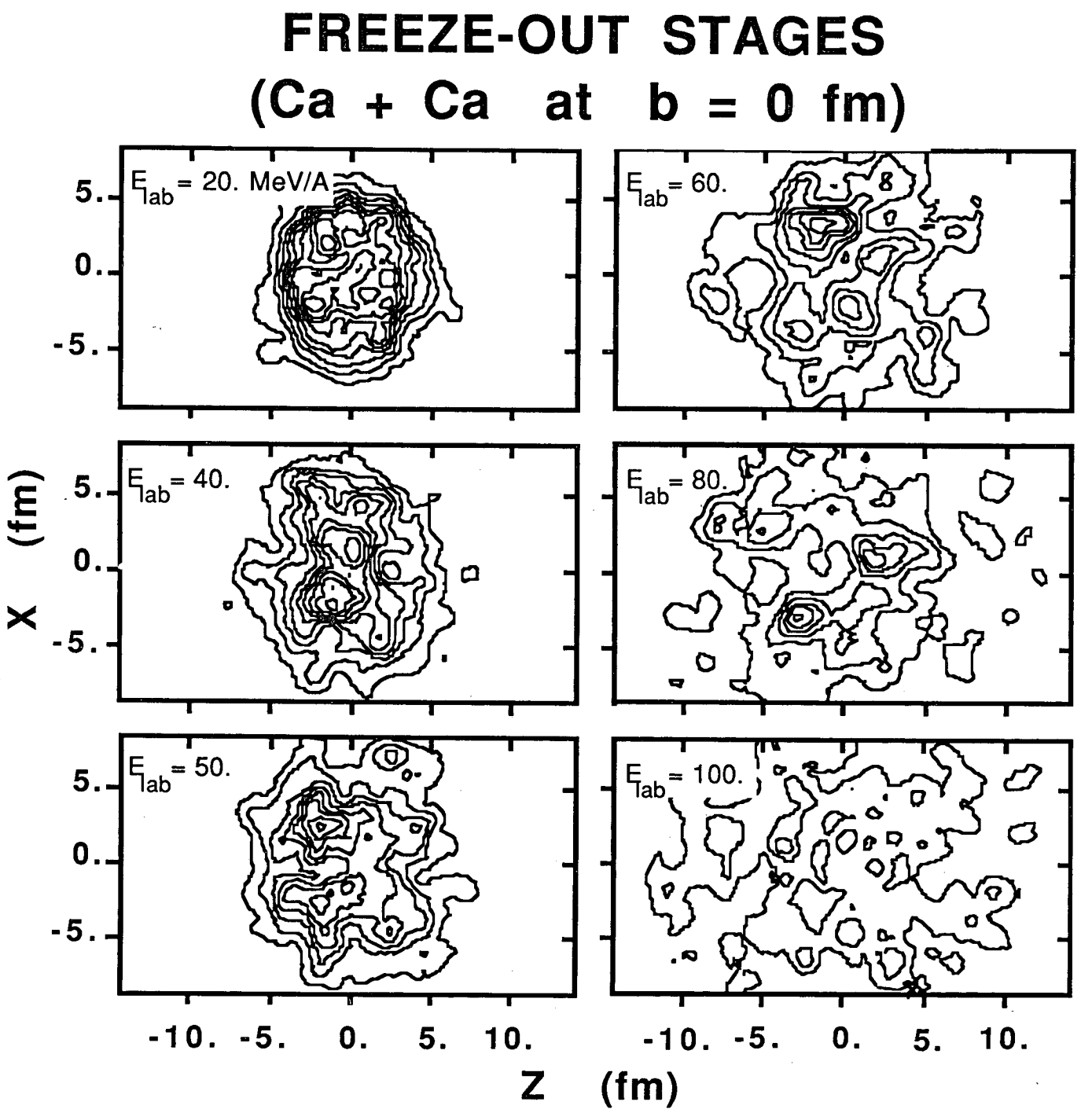
FREEZE-OUT STAGES
(Ca + Ca at b = 0 fm)
E_lab = 20. MeV/A
E_lab = 60.
E_lab = 40.
E_lab = 80.
E_lab = 50.
E_lab = 100.
5.
0.
-5.
X (fm)
-10. -5. 0. 5. 10.
Z (fm)

Figure 3

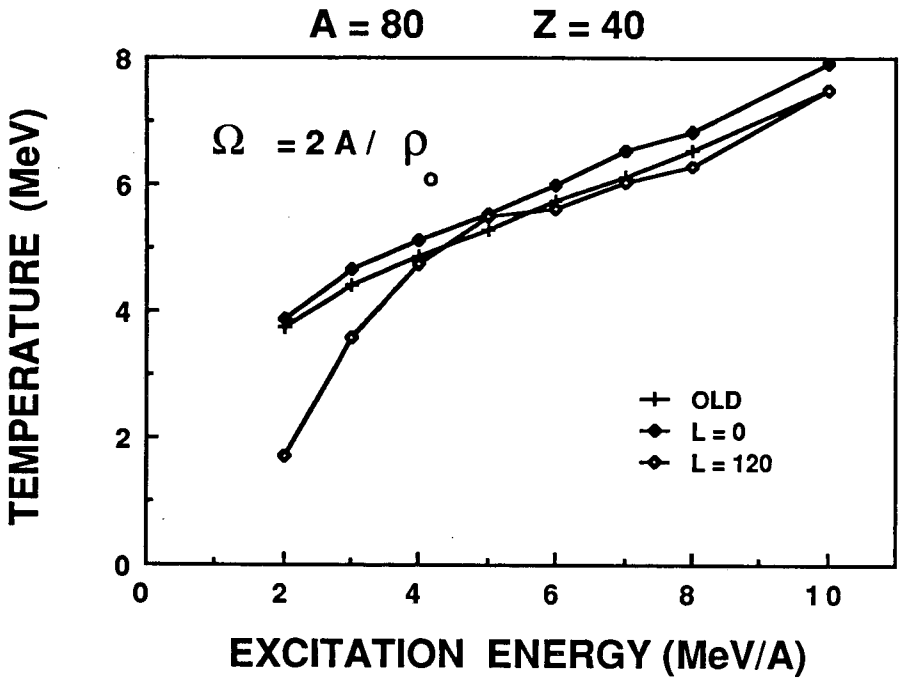

Figure 4a

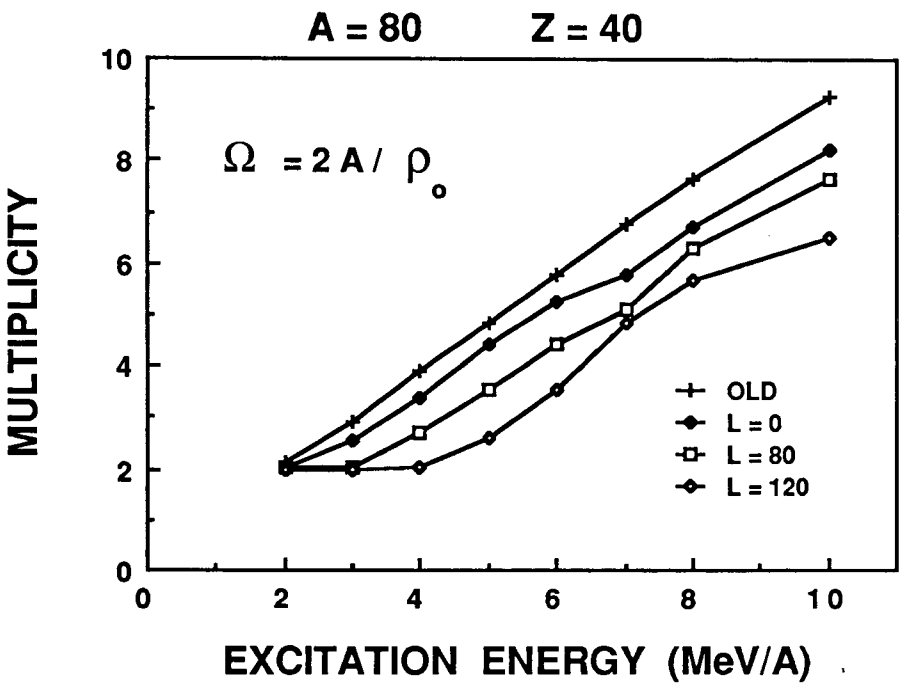

Figure 4b

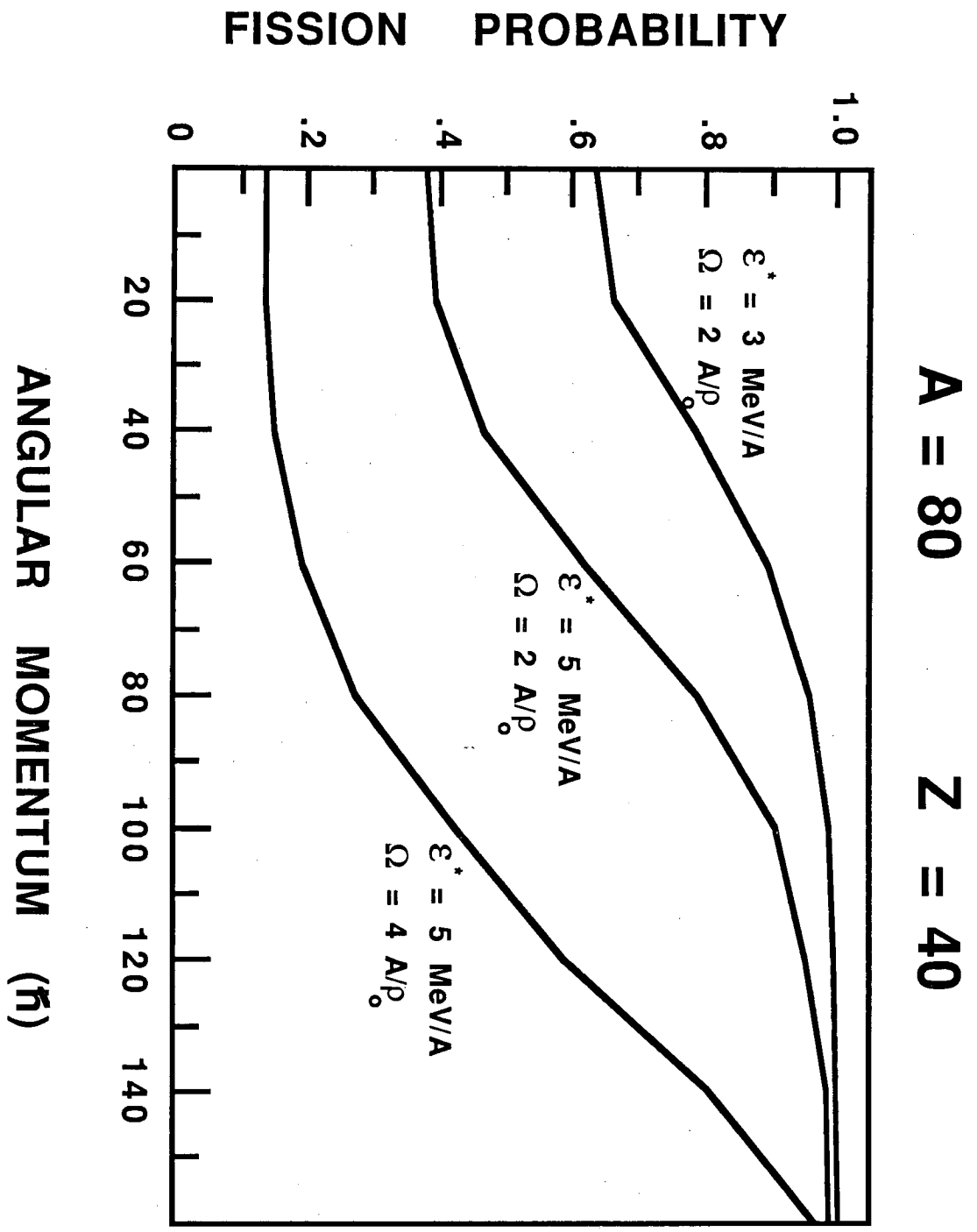
FISSION PROBABILITY
A = 80 Z = 40
ε* = 3 MeV/A
Ω = 2 A/ρo
ε* = 5 MeV/A
Ω = 2 A/ρo
ε* = 5 MeV/A
Ω = 4 A/ρo
0
.2
.4
.6
.8
1.0
20
40
60
80
100
120
140
ANGULAR MOMENTUM (ħ)

Figure 5

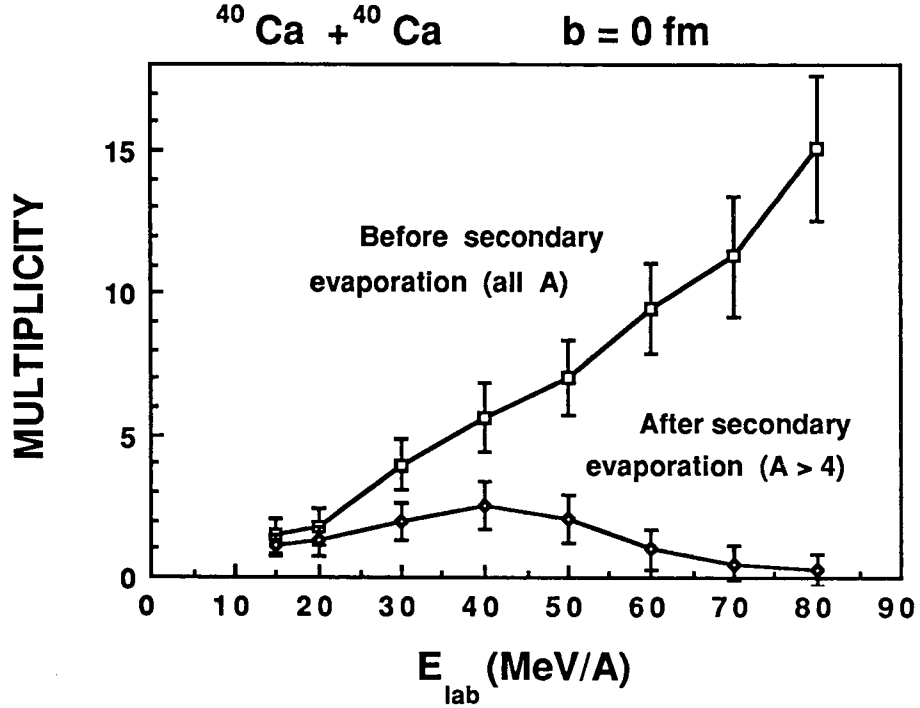

Figure 6a

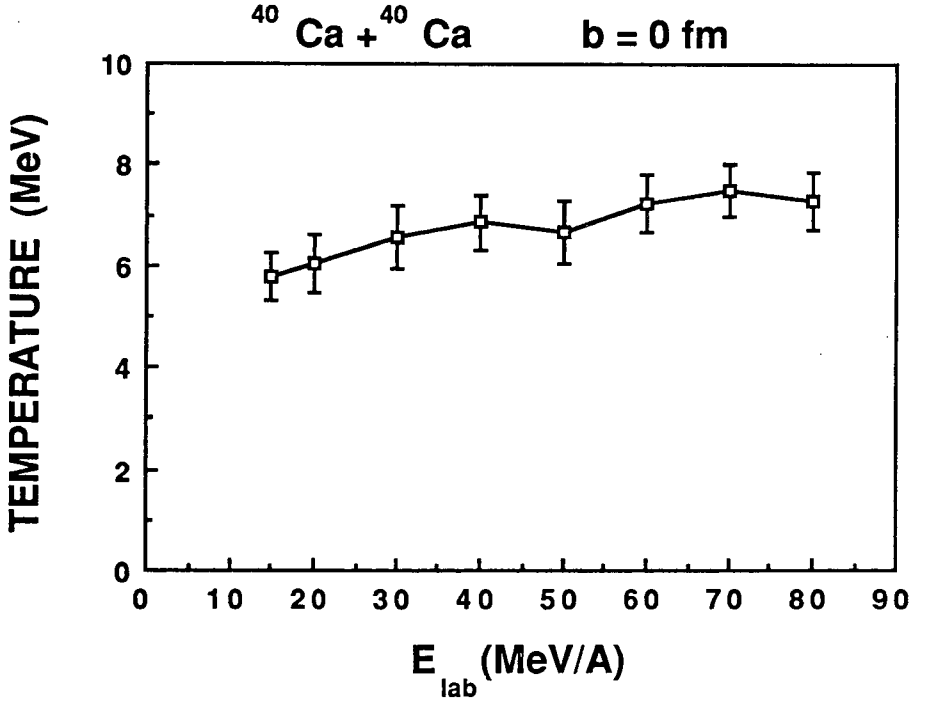

Figure 6b

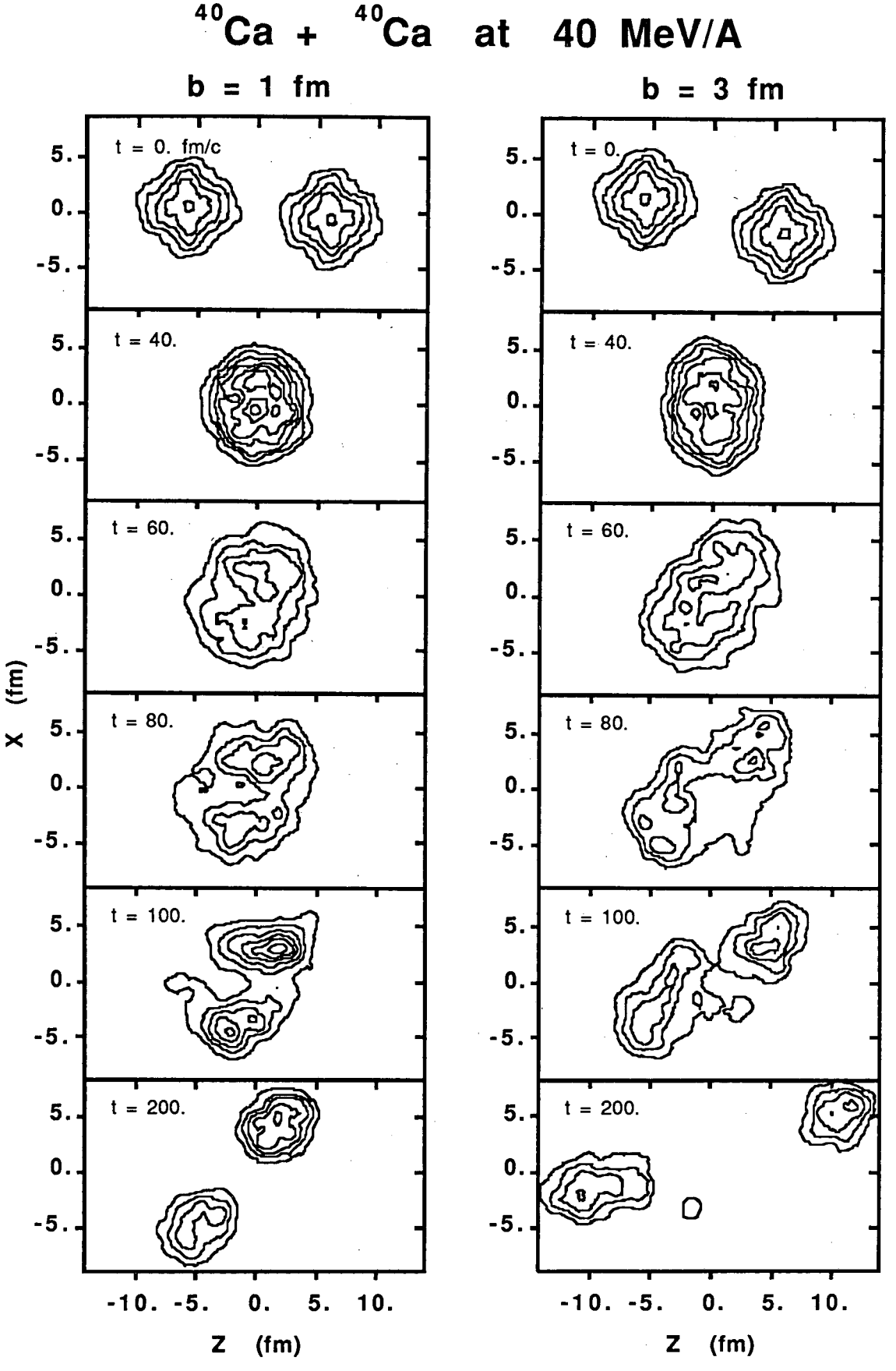
^{40}Ca + ^{40}Ca at 40 MeV/A
b = 1 fm
b = 3 fm
t = 0. fm/c
t = 0.
t = 40.
t = 60.
t = 80.
t = 100.
t = 200.
X (fm)
Z (fm)
5.
0.
-5.
-10.
-5.
0.
5.
10.

Figure 7

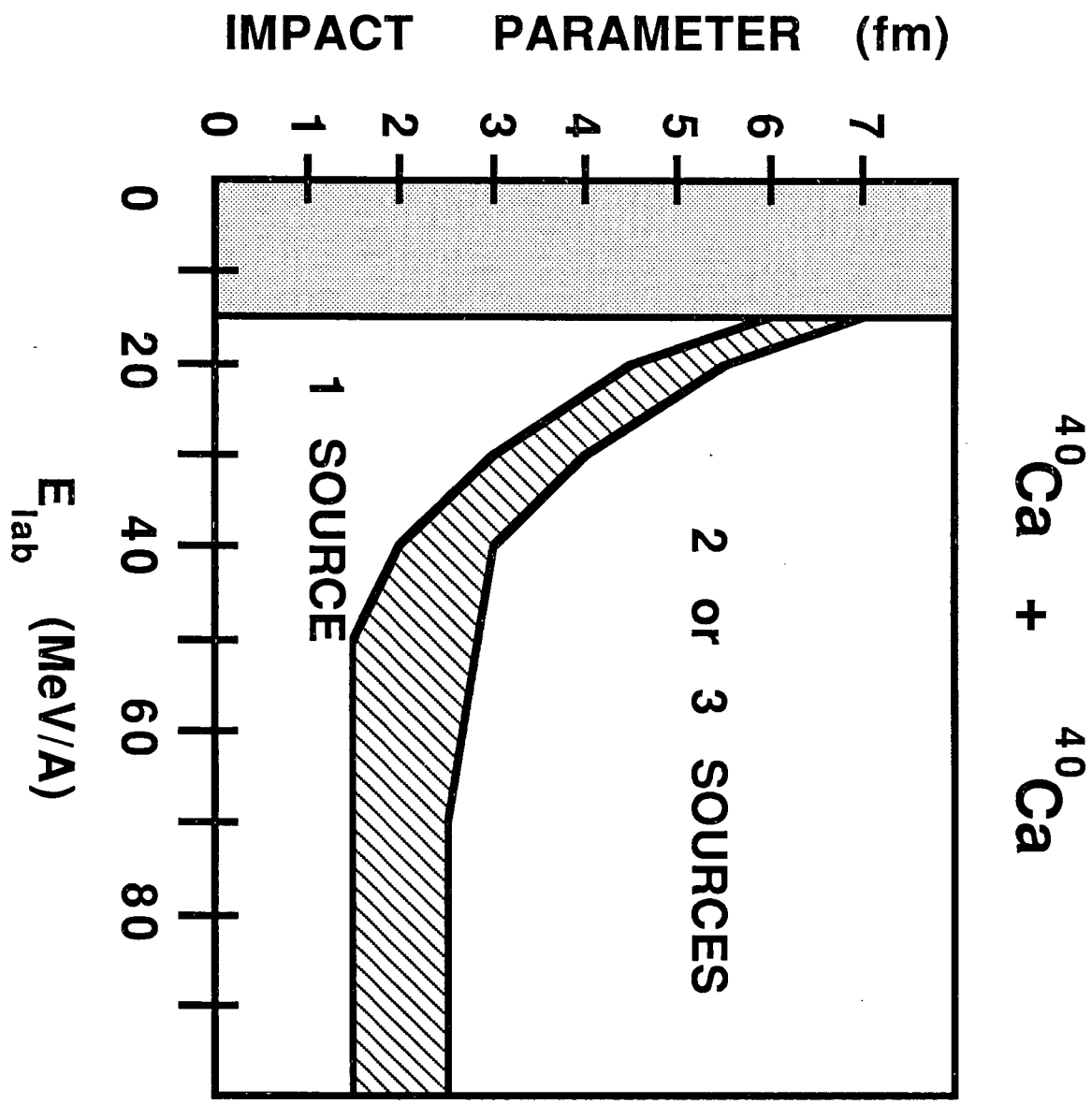
IMPACT PARAMETER (fm)
0
1
2
3
4
5
6
7
0
20
40
60
80
E lab (MeV/A)
1 SOURCE
2 or 3 SOURCES
40Ca + 40Ca

Figure 8

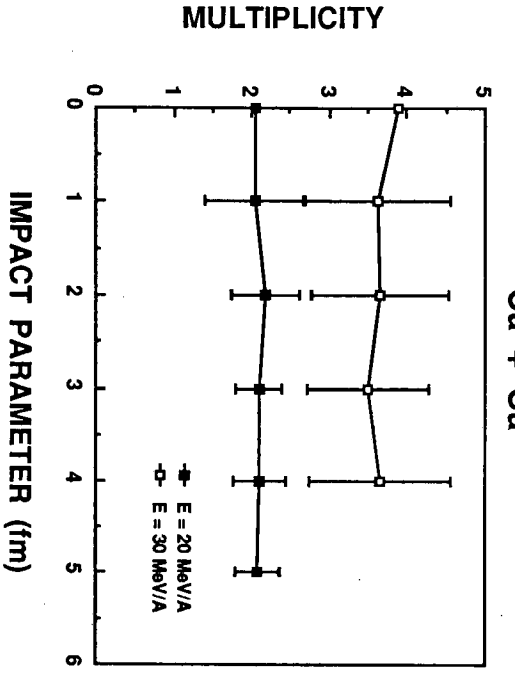

Figure 9a

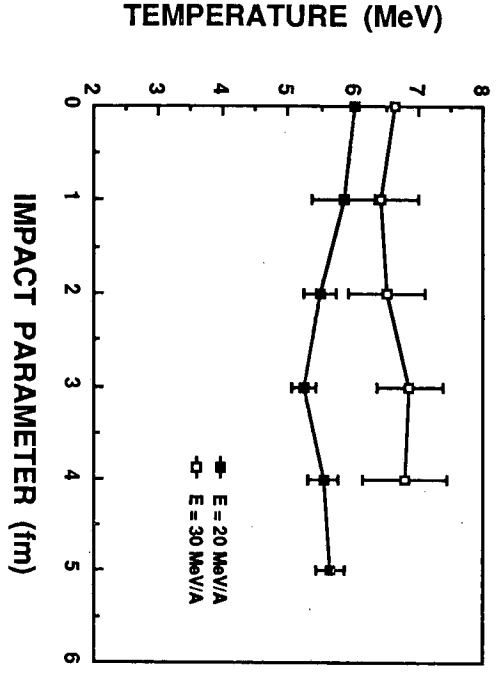

Figure 9b

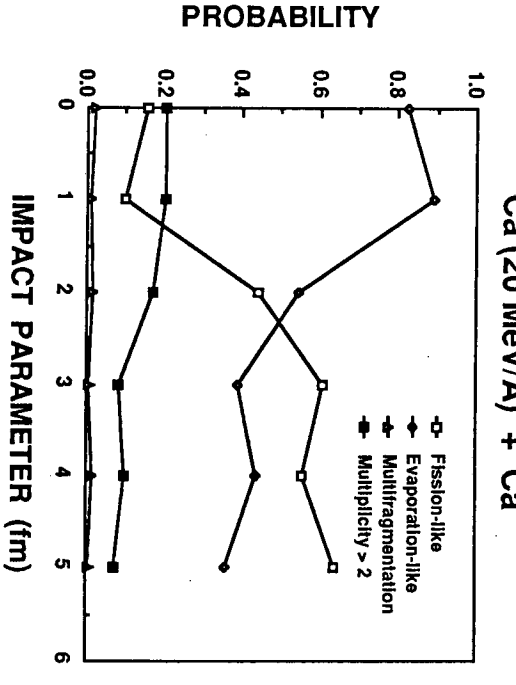

Figure 9c

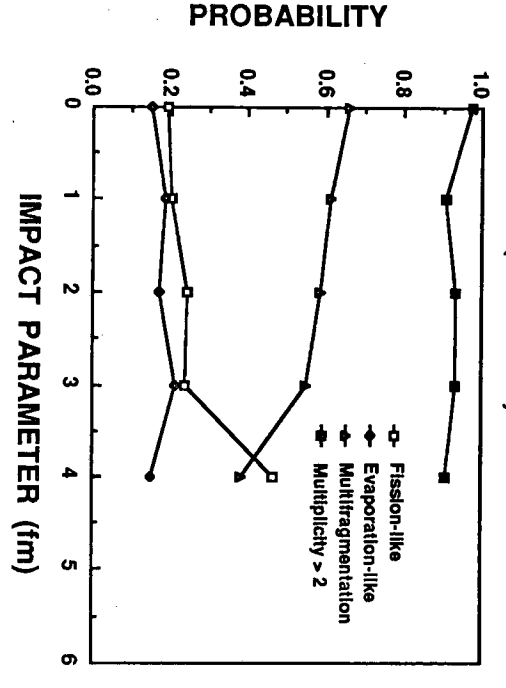

Figure 9d

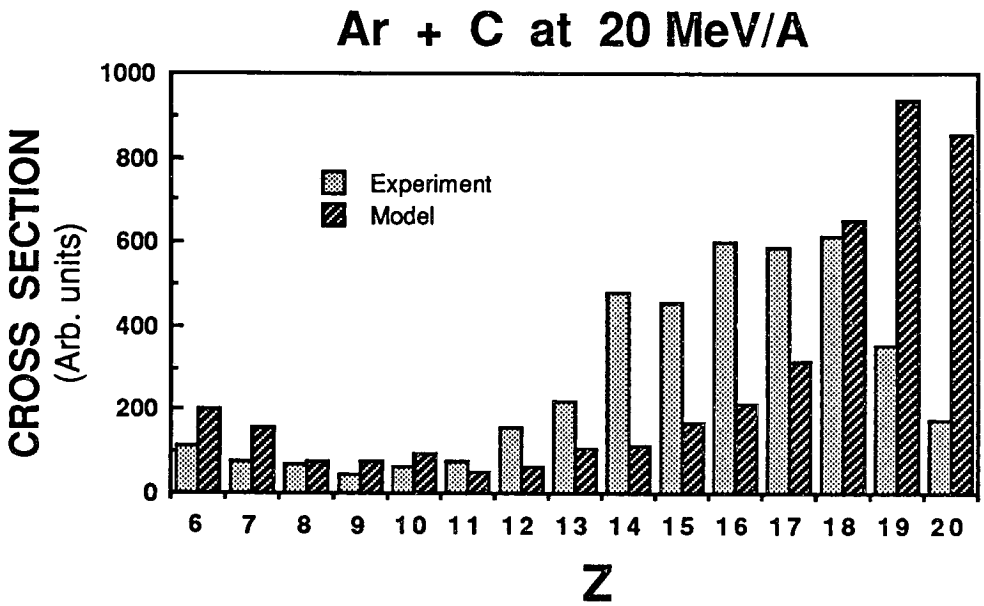

Figure 10a

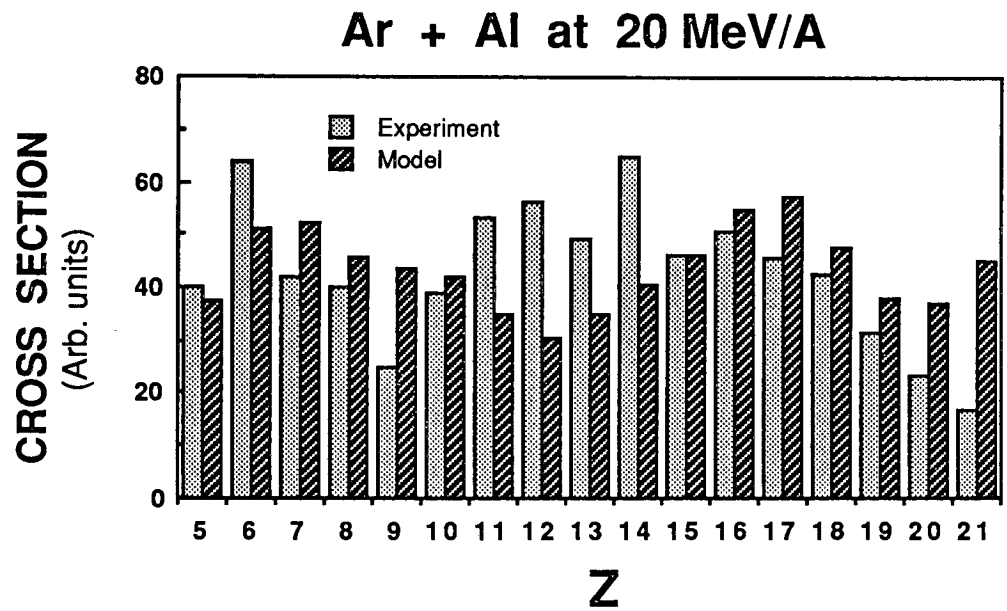

Figure 10b

LAWRENCE BERKELEY LABORATORY
TECHNICAL INFORMATION DEPARTMENT
UNIVERSITY OF CALIFORNIA
BERKELEY, CALIFORNIA 94720